

DRYING OF FOOD PRODUCTS BY SOLAR ENERGY

KARAM M. El-Shazly

Ass. Prof., Faculty of Engg., Shoubra, Zagazig University

Abstract

A nonmechanical solar dryer based on convective heat and mass transfer has been constructed to investigate the drying characteristics of various products such as grapes, onion and okra, using a simple solar dryer with forced ventilation for the case of onion and grapes solar drying or natural ventilation for the case of okra solar drying where solar heating is achieved by radiation and convection heat transfer. The dryer is constructed from locally available materials and operates on solar energy. Different tests were conducted for loading and unloading. The configuration is modeled and the simulation results are obtained. The model is verified by comparing the simulation results with the experimental data. The moisture loss during the drying process can be described by a general equation of the form $dM/dt = -cM$. The drying constants c_1 and c_2 for the constant and falling rate periods are calculated. Grapes and onion have constant and falling rate periods, while okra has only falling rate period.

1. INTRODUCTION

Solar energy is plentiful during the harvest season in EGYPT and there is urgent need for better utilization of solar energy to hasten agricultural drying to reduce spoilage and to improve the quality of the products. A typical locality in EGYPT may have a maximum solar intensity of about 950 W/m^2 and a total incident energy per day of about 30 MJ/m^2 [1]. Since the crops dryers are usually used for food and seed, the drying process could be done at the temperatures above the ambient temperature and the simple techniques could be adopted to collect the solar energy. There is sufficient information available that can be used to design workable solar dryers for various crops [2]. Several models have been proposed [3] for analyzing the drying phenomena of the agricultural products in thin layers.

Garge, H. P. et al [4] studied the effect of some parameters like air temperature, humidity and air flow rate on the drying of timber.

Alkathiri and Gentechev [5] conducted an experiment on solar drying of apricot. The aim of experiment is to investigate the possibility of using low cost dryer with product having good chemical and microbiological characteristics.

Hegazy and Mousa [6] conducted the performance of improved-design cabinet-type solar dryers with parallel and horizontal absorber plates. For each orientation, parametric variations of the minimum spacing between the absorber plate and the glass cover were made. The performance enhancement was accentuated at smaller values of gap minimum spacing and incorporating an absorber plate parallel to

the glass cover. The average gap spacing should be in the range of 65-70 mm for optimum performance.

Shomo S. Ali [7] conducted the drying of okra at humid conditions in thin layers and being evaluated at different air flow rates. The solar drying analysis is generally complicated not only due to fluctuation of the different drying parameters but also to the interaction between them. The most important parameters affecting the drying rate are the external factors such as the moisture content and the nature of the material physical structure and chemical composition and the way in which the material is prepared- shape, size and loading.

A simple low cost and nonmechanical solar dryer has been designed, constructed and tested. Simulation model is developed for a simple dryer configuration and the performance is evaluated. The validity of the model is tested and the temperature rise can be predicted for different collector areas and flow rates. The drying constants for the constant and falling periods are determined.

2. PSYCHROMETRICS AND DRYING PROCESS

A psychrometric chart is used to determine moist-air drying properties. There are relationships existing between the relative humidity (ϕ), product moisture content M and drying air temperature. A volume of air is heated in the solar collector having porous medium and passed through a fixed bed of a thin layer of the sample which is dry chamber by forced or natural convection to accomplish dehydration by evaporation. In the case of drying by natural convection the difference in density between heated and unheated air creates the pressure gradient required to cause the heated air flowing without any external power source. The dryer is intended to dry 5Kg of any crop as a sample from an initial moisture content M_i (wet basis) to an equilibrium moisture content M_e of 15% or less.

From psychrometric chart as shown in Figure (1), if ambient air temperature is equal to 32.5 °C and relative humidity equal to 80% is heated to 50°C, then relative humidity is reduced to 30%. If this heated air is used to remove moisture from a thin layer of the sample, the adiabatic evaporation continues along a line of constant wet bulb temperature (B-C) until an intersection with the saturation curve of $\phi_c = 90\%$ is reached, and drying air temperature is reduced to $T_c = 34^\circ\text{C}$. The fall in temperature from B to C represents the maximum amount of heat available for evaporation of water per Kg of dry air circulated. The humidity ratio W changes from 0.024 to 0.031 and $\Delta W = 0.007$ means that the drying capability of heated air is 7 times greater than for unheated air (path AD).

3. THEORETICAL ANALYSIS

From Figure (1) the mass of water evaporated m_w and absorbed by a mass of drying air m_a is related by

$$m_w L = m_a C_a (T_B - T_C) \quad (1)$$

where L is the latent heat, C_a is the specific heat of air.

If m_f is the final mass of sample when a quantity of water m_w has been removed, m_i is the initial mass of wet sample and m_d is the mass of the completely dried sample, then, on wet basis, the initial moisture content is

$$M_i = \frac{(m_i - m_d)(100)}{m_i} \quad (2)$$

and the final moisture content

$$M_f = \frac{(m_f - m_d)(100)}{m_f} \quad (3)$$

Since $m_w = (m_i - m_f)$, then

$$m_w = \frac{m_i (M_i - M_f)}{(100 - M_f)} \quad (4)$$

The basic energy equations for the plate and glass cover of the collector are as follows[8]

Energy equation for the plate (no wire netting)

$$[(A_p)q_s](1-f_{dl})(1-f_{sh})=q_{c,p-g}+q_{r,p-g}+q_l \quad (5)$$

Energy equation for the glass cover:

$$q_{c,p-g}+q_{r,p-g}+q_{ab} = q_{c,g-w}+q_{r,g-sk} \quad (6)$$

The energy equation for the air at a distance X from entrance to collector is

$$mc_a \frac{dT_a}{dx} = h_p w_p (T_p - T_a) - h_c W_g (T_a - T_g) \quad (7)$$

It should be noted that q_s is the total radiation as measured by a solar pyranometer. For clear days as it is the case in Egypt, the scattering of solar radiation is mostly forward scattering with most of the radiation coming from the direction of the sun. Then the angular correction factor to be applied to the diffuse radiation is therefore the same as that for beam radiation [9].

The first and the second terms on the R.H.S. of Eq.(5) are the convective and radiative heat transfer between plate and cover respectively. The first and second terms on the R.H.S. of Eq.(6) are the convective heat transfer between cover and wind and radiative heat transfer between cover and sky respectively.

The values of radiative heat transfer coefficients between plate and cover and between cover and sky are respectively:

$$h_{r,p-g} = \frac{\sigma(T_p^2 + T_g^2)(T_p + T_g)}{\frac{1}{\epsilon_p} + \frac{1}{\epsilon_g} - 1}$$

$$h_{r,g-sk} = \frac{\epsilon_g \sigma(T_g^2 + T_{sk}^2)(T_g + T_{sk})(T_g - T_{sk})}{(T_g - T_{am})}$$

The sky temperature is a function of ambient temperature. The basic equations for determining the convective heat transfer coefficients from plate to air and from air to cover are [10]:

Heat transfer coefficient between plate and air

$$\begin{aligned} \text{Nu} &= 0.54 (\text{Ra})^{0.25} && \text{Laminar flow} \\ \text{Nu} &= 0.014 (\text{Ra})^{0.33} && \text{Turbulent flow} \end{aligned}$$

Heat transfer coefficient between air and glass cover

$$\text{Nu} = 0.8 (\text{Ra})^{0.25} \left[\frac{\cos \phi}{1 + \left(1 + \frac{1}{\sqrt{\text{Pr}}}\right)^2} \right]^{0.25}$$

From equations (1),(5),(6) &(7), one can obtain the values of plate temperature, air temperature at outlet of the collector, air temperature at outlet of the dryer and cover temperature. A computer program was written to solve the governing equations on the electronic computer, one can obtain the simulation results.

4.CONSTRUCTION OF DRYER AND MONITORING

A major design consideration was to select and use locally available materials to build the dryer. The dryer is shown in Fig. (2).

A single layer of glass was used as glazing cover for the solar collector, its area is 2m^2 , it was tilted at 30° and was supported to protect against wind fatigue with a 10 cm air channel between glazing and absorber. The air channel is filled with porous medium (wire netting) to enhance the heat transfer due to increase the heat transfer coefficient in the case of using porous medium than that of excluding porous medium.

Trays were used for easy loading and unloading the materials to be dried. Five food trays were incorporated into the chamber, each made of a layer of wire mesh to pass hot air through agricultural crops and the area of each is 0.5m^2 . Three sides of the drying chamber are thermally insulated, one of them has two back doors which are use to load the solar dryer, while the fourth side is glass. The peel of onions is removed and sliced manually. Grapes were immersed in the olive oil and water before spreading on the drying trays to increase the water permeability of the waxen coat. Okra is sliced when its size is large.

One kitchen fan of 100 Watt is used in the dryer. It is mounted at the outlet of the drying chamber and the inlet of the chimney.

Copper-constantan thermocouples connected with amplifier were used to measure dry and wet bulb temperatures at inlet and outlet of the air collector and outlet of the chimney.

Solar meter is used to measure intensity of solar radiation and calibrated fan is used to measure the air velocity at the outlet of the chimney.

5. MODEL VERIFICATION.

The simulation results which obtained on the electronic computer are compared with the actual experimental measurements to verify the validity of the present model. The experiments were taken on the dryer. The plate area of the dryer is 2m^2 .

Table (1) gives a comparison at different time of day between simulation results and experimental data for air temperatures at outlet of the collector(T_2) and outlet of the dryer(T_3) at mass flow rate 0.04Kg/s . The predicted values of air calculated at absorptivity of plate equals 0.9. Comparing the simulation and measured results of (T_2) and (T_3), it will be seen that the agreement is good. The discrepancy which exists between them can be attributed to:

- (a) Solar collector with wire netting for experiments, while that without wire netting for model.
 - (b) The inherent errors in measuring temperatures.
 - (c) The discrepancy which might exist between the assumed and actual values of the optical characteristics of the plate and glass cover of the collector
- However, the closeness of the agreement gives confidence of the model.

6. RESULTS

In general the drying rate is a function of many parameters such as relative humidity, air flow rate, the material moisture content, the temperature and the effective solar drying period. Most of these parameters are related and interact to each other.

Figure (3) shows the variation with time each of solar intensity, dry bulb temperatures at the inlet and outlet of the collector and outlet of the dryer for two cases which are loading and unloading. The flow of air through the dryer is forced and the material which dried is onion. This figure shows the difference in temperature between inlet and outlet of the dryer (t_2-t_3) is smaller for the case of unloading than the case of loading ($T_2 - T_3$). This is due to the fact that the heat is transferred from heated air to the agricultural crops.

A typical diurnal variation of temperatures in the dryer with loading by onion is recorded on September. At mid day, the maximum temperature at the outlet of the collector is 60°C .

Figure (4) shows the variation with time each of solar intensity, dry bulb temperatures at the inlet and outlet of the collector and outlet of the dryer for two cases which are loading and unloading. The flow of air through the dryer is natural and the material which dried is okra. A typical diurnal variation of temperatures in the dryer with loading by okra is recorded on September. At mid day, the maximum temperature at the outlet of the collector is 85°C . The maximum temperature in the case of natural convection though the collector is greater than that for the case of forced convection. This is due to the fact that the rate of mass flow in the case of natural convection is smaller than that for the case of forced convection. When the mass flow rate of air decreases, the outlet temperature of the collector increases and the drying time decreases. Porous medium enhances the coefficient of heat transfer specially for small density which is 4 Kg/m^3 . As the density is small, the porosity is

large. This tends to increase the heat transfer coefficient when the flow of air follows Darcian natural convection.

Figure(5) shows the variation of simulation results at different mass flow rates. As mass flow rate increases, the air temperature at outlet of the collector decreases. This is expected for increasing the velocity of air through the collector.

Figure(6) shows the variation of simulation results with collector area for a typical day in September at noon time. Simulation results have been obtained for different mass flow rates. As collector area increases, air temperature at the collector outlet increases.

Figure (7) shows the moisture content variation with drying time. As drying time increases, the moisture content decreases. This is due to the fact that the weight of the specimen decreases with increasing drying time. These curves for drying process can be represented two straight lines with a short curved transition. The short period AB is the constant rate period where moisture is removed at a uniform rate until the critical moisture content is reached. During this period the wet surface of the product behaves as a free water surface and the period continues as long as water is supplied to the surface as rapidly as evaporation takes place. This period is encountered in the case of drying onion and grapes. The period BC for onion and grapes is the falling rate period where the rate of moisture removal decreases and is characterized by subsurface evaporation. Most of the drying actually takes place in the falling rate period and involves the movement of moisture within the material to the surface and removal of the moisture from the surface. The drying of okra encountered no constant rate drying period. This was to be ascribed to the colloidal and hydrophilic nature of the okra which causes the water molecules to be held more tightly and to the surface deformation caused by shrinkage.

For the thin layer drying investigation, the graph of figure (8) shows that the drying process can be represented by an equation of the form $dM/dt = -cM$, where c is the drying constant which can be evaluated for constant rate period (as c_1) and the falling rate period (as c_2). Table (2) gives the drying parameters for the various samples with higher c values would be dehydrated in a shorter period under identical conditions.

For the constant rate period, the drying rate is proportional to the free moisture content i.e

$$\frac{dM}{dt} = -c_1 (M - M_c)$$

and

$$\int_{M_i}^{M_c} \frac{dM}{(M - M_c)} = \int_0^{t_c} c_1 dt$$

or

$$\frac{(M(t) - M_c)}{(M_i - M_c)} = \text{Exp}(-c_1 t_c)$$

Similarly, the drying equation for the falling rate period is

$$\frac{(M(t) - M_e)}{(M_c - M_e)} = \text{Exp}(-c_2 t_e)$$

The total drying time = $(t_c - t_e)$. The moisture loss can therefore be considered mathematically as an exponential decay, even though the physical mechanism of mass transfer consists of free water evaporation and bound water diffusion. The dehydration consists of two different mechanisms, the removal of free water in the cell cavities and of water films trapped within capillaries, adsorbed membranes in solution within cells or chemical bound with solids as water of crystallization.

7.CONCLUSIONS

Solar dryer is designed and constructed from locally available materials. In the light of the predicted performance of the dryer configuration, the use of solar energy for small scale drying in rural areas is feasible. The drying time for solar drying of a sample is about half time taken in open-air (sun) drying. The drying process is controlled by initial removal of free water followed by removal of bound water. Grapes and onion have constant and falling periods, while okra has falling period. An equilibrium moisture content of 15% is achieved naturally faster than forced convection in the case of using porous medium having density 4Kg/m^3 at the passage of air through collector. Food products were dried to a prescribed value of moisture content to preserve them for storage without the need for refrigeration.

NOMENCLATURE

A	Effective absorptance of the plate
c, c_1, c_2	Constants
C	Specific heat $\text{J/kg } ^\circ\text{C}$
f	Factor
h	Heat transfer coefficient $\text{W/m}^2 \text{ } ^\circ\text{C}$
$\text{mW/cm}^2 = 10 \text{ W/m}^2$	
m	Mass Kg
M	Moisture content
Nu	Nusselt number
Pr	Prandtl number
q	Heat flux W/m^2
Ra	Rayleigh number
T	Temperature
w	Width
Φ	Angle of inclination of glass cover
ϵ	Emissivity
σ	Stefan-Boltzmann Constant

Subscripts

a	air,	ab	absorbed,
am	ambient,	c	convective
r	radiative	s	solar
l	losses	g	glass
p	plate	w	wind
sk	sky	d	dust
sh	shading	i	initial
f	final	e	equilibrium
d	completely dried		

REFERENCES

- 1- S. H. Soliman, N. H. Helwa, `` Insolation Over EGYPT-Daily Totals of Solar Radiation at 23 Sites", Engineers (India), Vol. 64, part IDGE3, June, 1984.
- 2- A. Aensu and V. Asiedu-Bondzie ``Solar Drying With Convective Self-Flow and Energy Storage'', Solar and Wind Technology, Vol. 3, No. 4, pp. 273-279, 1986
- 3- D. H. Willits, I. J. Ross, `` A mathematical Drying Model for Porous Materials" Part 1, Theory, Trans ASME (556-562), 1976.
- 4- H. P. Garg and D. S. Hrishikeshan `` Solar Timber Drying-State of Art", Int. REC, Amman, Jordan, June 22-26, pp.335-352, 1992.
- 5-M. A. Alkathiri and L. N. Gentechev `` Solar Drying of Apricot " Int. REC, Amman, Jordan, June 22-26, pp. 323-334, 1992.
- 6- A. A. Hegazy and F. A. Mousa, " Improved Design for Natural Convection Cabinet Type Solar Dryer"; 1st Jordanian Mech. Eng. Conf., Amman, 25-28 June, pp 66-82, 1995
- 7- S. S. Ali, `` Solar Drying of Vegetables in Humid Environment", Int. REC, Amman, Jordan, June 22-26, pp. 311-322, 1992
- 8- M. M. El-Sayed, I. S. Taha & J. A. Sabbagh,"Design of Solar Thermal Systems", Scientific Publishing Center, King Abdulaziz University, Jeddah, 1994.
- 9- J. A. Duffie and W. A. Beckman,"Solar Energy Thermal Process", John Wily and Sons, New York, 1980.
- 10- H. Y. Wong,"Heat Transfer For Engineers" Long man, New York, 1977.

TABLES

Table(1) Measured and calculated values for air temperatures at outlet of the collector(T2) and outlet of the dryer(T3).

Time	Experimental Results		Simulation Results	
	T2	T3	T2	T3
11 Am	47.5	42.5	46.5	40.5
11.5 Am	53	36	47.7	41.8
12 noon	57.5	42.5	49.5	43.7
12.5 pm	60	42.5	50.5	44.6
1 pm	60	45	51.6	45.8
1.5 pm	60	42.5	52.4	46.5
2 pm	57.5	42.5	51.5	45.7
2.5 pm	55.5	42.5	51.2	45.3
3 pm	54	41.5	49.7	43.9

Table 2. Drying characteristics of agricultural crops
(t_e =time to attain M_e , t_c =time to attain M_c)

Sample dried	Moisture Content %			Drying time h		Drying constants (1/h)	
	M_i	M_c	M_e	t_e	t_c	c_1	c_2
Grapes	81	57	15	20.5	4.5	0.078	0.067
Onion	79.8	55	15	15	3.5	0.106	0.090
Okra	80	---	15	11.5	---	---	0.146

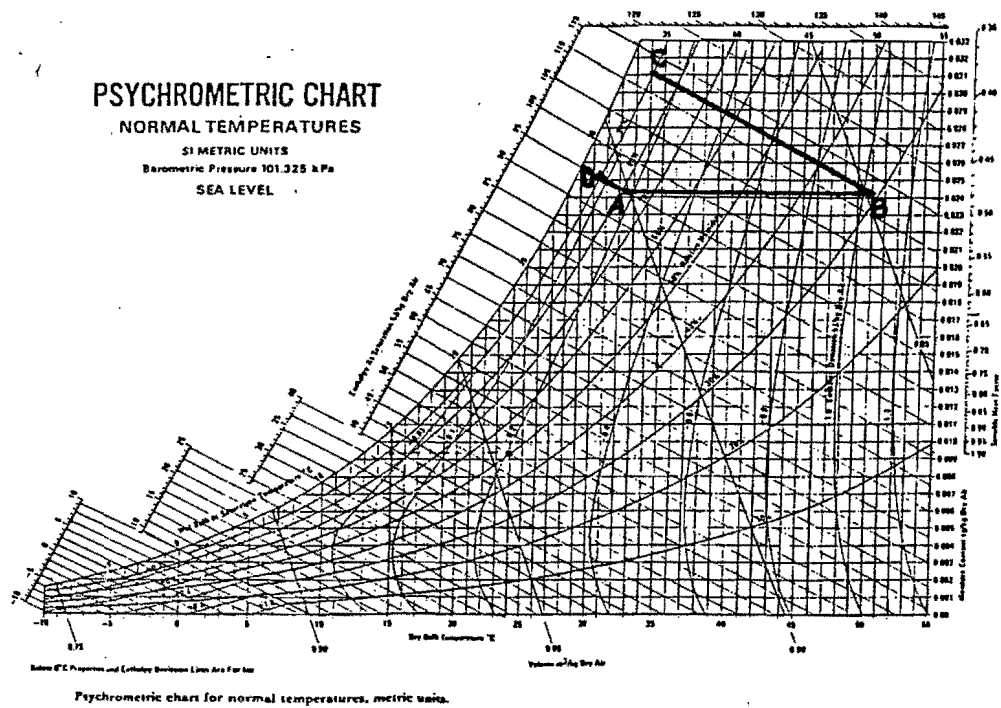


Fig.(1): Psychrometric chart for normal temperatures, metric units

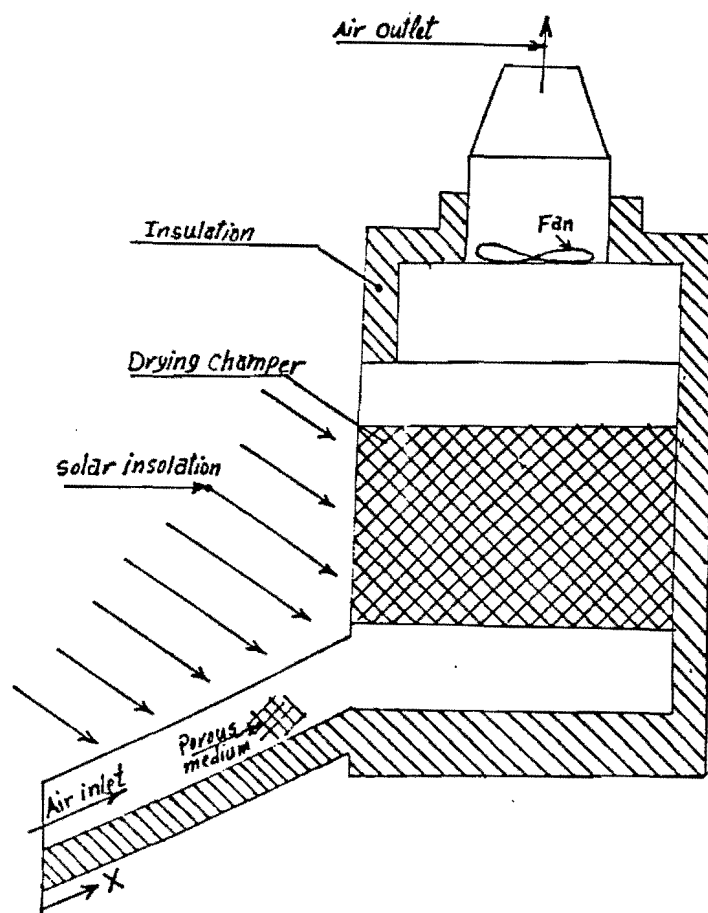


Fig.(2): Cross section for solar dryer.

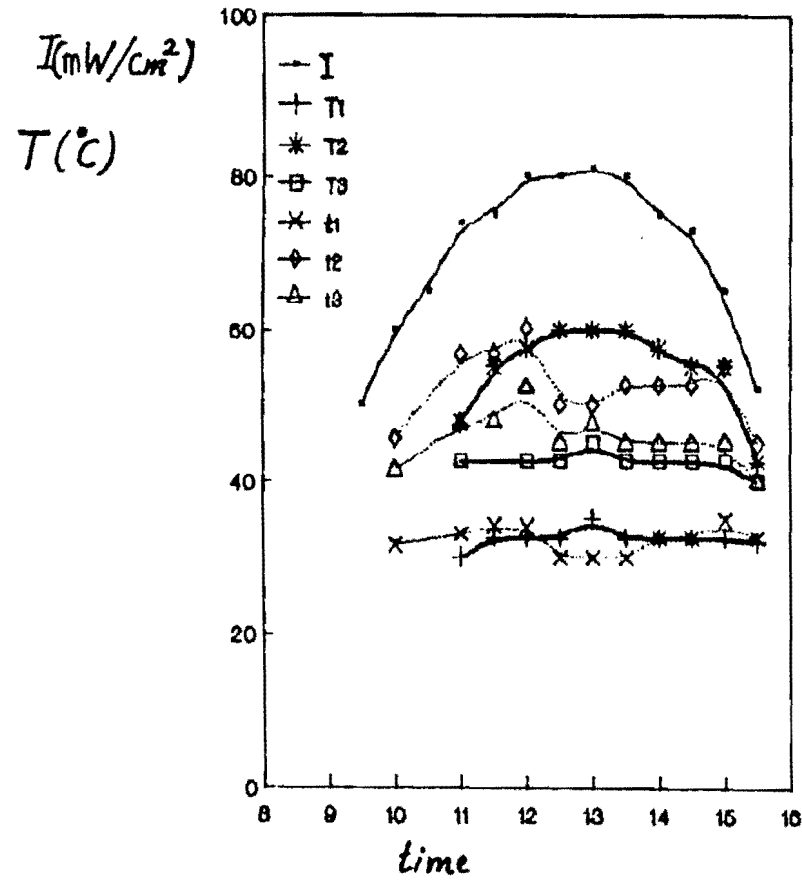


Fig.(3): Variation with time each of (—■—) solar intensity, I, temperatures at inlet and outlet of the collector and outlet of the dryer for drying onion for two cases (—) loading and (— · — · —) unloading.

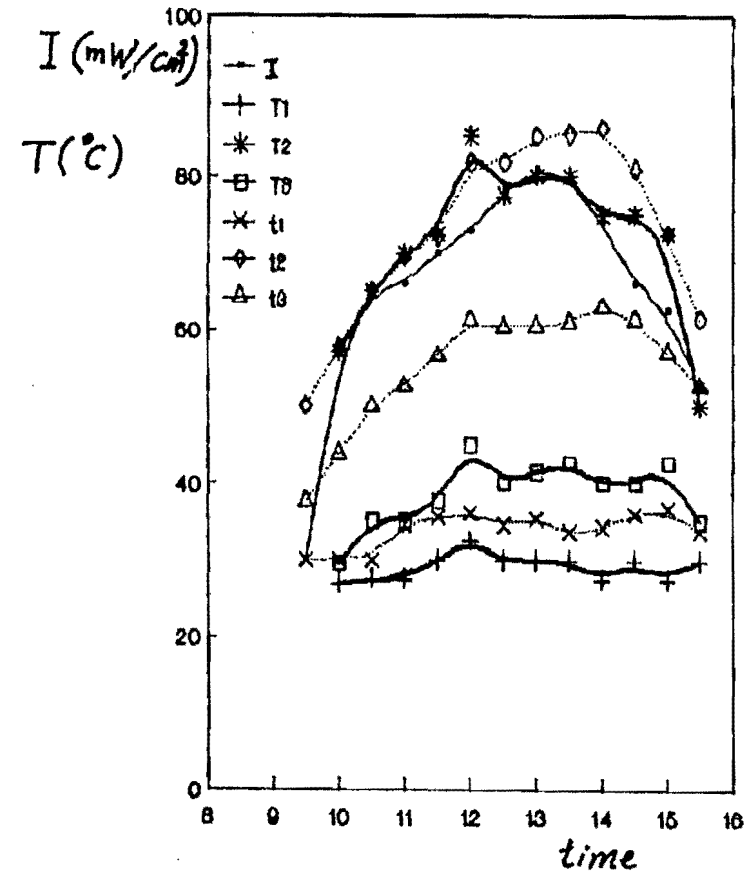


Fig.(4): Variation with time each of (—■—) solar intensity, I, temperatures at inlet and outlet of the collector and outlet of the dryer for drying okra for two cases (—) loading and (— · — · —) unloading.

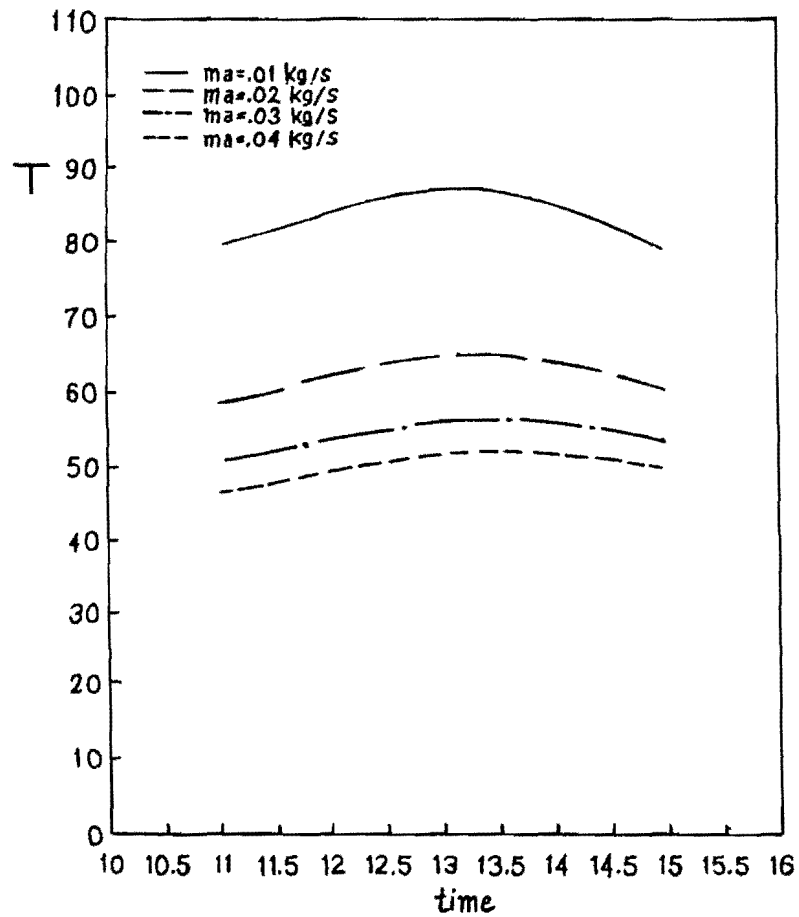


Fig.(5): Variation of air temperatures at outlet of the collector with time for different mass flow rates

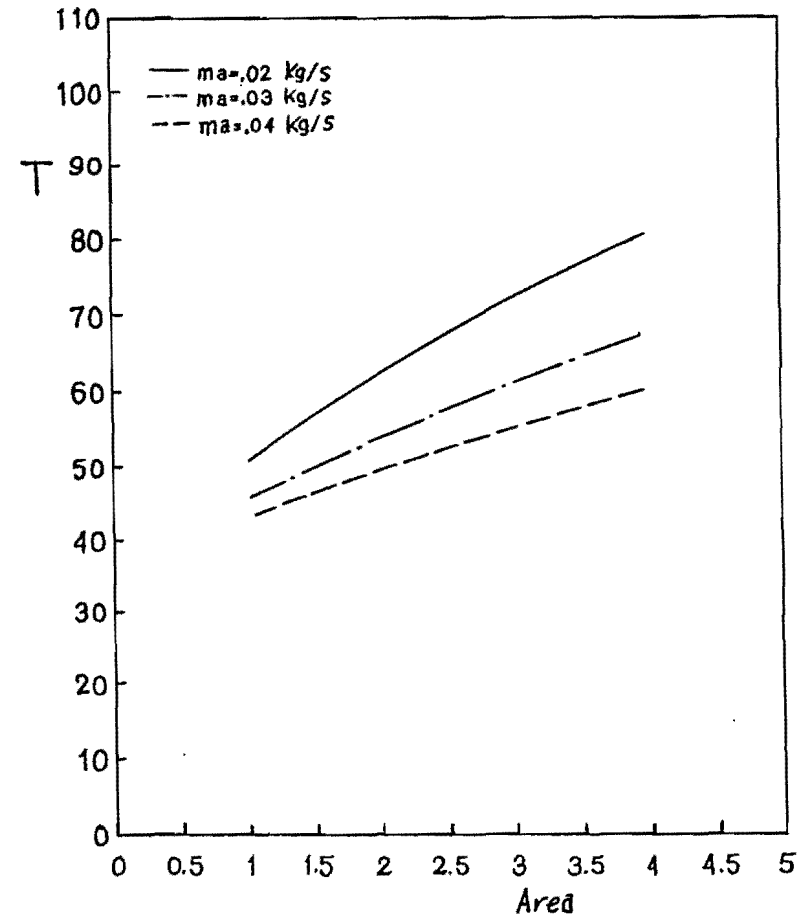


Fig.(6): Variation of air temperatures at outlet of the collector with collector area in September at noon for different mass flow rates

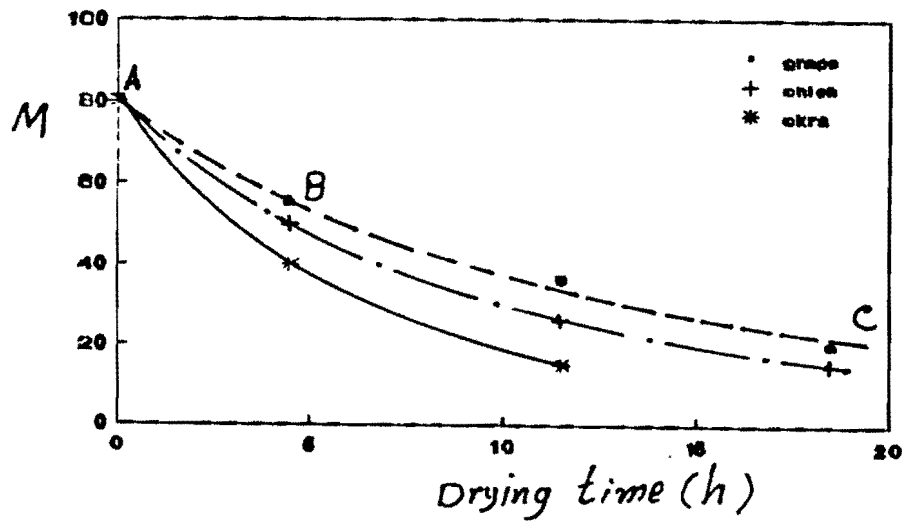


Fig. (7): Variation of moisture content with drying time for (---) grapes, (— · —) onion and (—) okra.

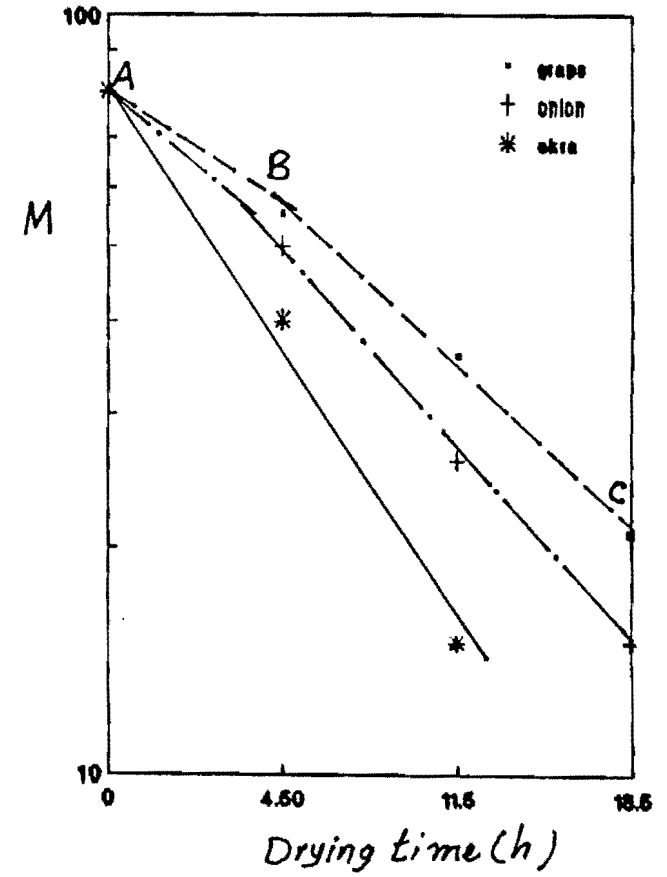


Fig. (8): A log linear plot of moisture loss to illustrate constant rate and falling rate periods of drying.